Int. Journ. of Laser Science, Vol. 1, pp. 253–264
Reprints available directly from the publisher.
Photocopying permitted by license only.

Analysis of the Nonequilibrium Heat Transport Time of Electrons in Cu Films Irradiated by a Femtosecond Laser Beam

X. F. Xu[1,2,*], X. L. Li[1], Q. W. Wang [1], F. F. Yang[1] and Y. F. Gao[1]

[1]*School of Mechanical Engineering, Jiangsu University, Zhenjiang 212013, Jiangsu Province, China*
[2]*School of Mathematics and Physic, Suzhou University of Science and Technology, Suzhou 215000, Jiangsu Province, China*

The finite element method (FEM) is used to simulate the changes of electron temperature and lattice temperature in Cu films during the femtosecond laser pulses heating. The simulation results show that during the electron nonequilibrium relaxation time, the full width at half maximum (FWHM) time of the electron temperature will rise with the increase of the pulse number, the width and pulses interval; however, the electron nonequilibrium relaxation time is independent of both the pulses interval and pulse width, but increased with the number of excitation pulses. By the laser heating with the four pulses of 300 fs, and the pulses interval of 520 fs, the FWHM time of electron temperature is 5.6 ps, and the electron nonequilibrium relaxation time is 15 ps. Compared with the single pulse heating that the FWHM time of electron temperature is 1 ps, and the electron nonequilibrium relaxation time is 8 ps, they have been significantly improved.

Keywords: Femtosecond laser, copper, Cu, films, electron temperature, lattice temperature, electron nonequilibrium relaxation

1 INTRODUCTION

The main application of femtosecond laser in industry is femtosecond laser processing [1], such as femtosecond laser cutting [2, 3], femtosec-

*Corresponding author: E-mail: xuxf@yahoo.com

ond laser drilling [4, 5]. The outstanding advantage is that there is almost no heat affected areas during femtosecond laser processing [6, 7]. This process, however, only occurs in the nonequilibrium conduction duration of the electronic temperature. Here, the heat which is produced by the laser heating is diffused faster in the air than diffused into the crystal lattices, the lattice temperature remains low, so there is almost no thermal effect.

The ablation of the metal film by femtosecond laser pulse is a nonequilibrium thermal process and the process duration is extremely short - less than several picoseconds, so a single femtosecond pulse cannot make the laser processing efficiently. So, in actual industrial processing, people are usually using femtosecond laser pulses with high repetition frequency. In such instances the pulse interval of the femtosecond laser is much greater than the electron photon relaxation time; consequently, the electron and lattice temperature can be approximated in the state of thermal equilibrium because at this condition, the action of the laser beam heating metal films is similar to the process of equilibrium thermal conduction. With the increase of the number of pulses, the thermal effect is more serious: both the stress, the crack and the roughness of the ablated edge are increased and so the processing effect is worse [8, 9].

In order to solve the problem of the short electron nonequilibrium relaxation time, a number of femtosecond laser pulses with a certain time interval are used. By designing the femtosecond laser pulses sequence, it can significantly extend the electron nonequilibrium relaxation time, so the thermal effect in the laser heating process will be effectively suppressed, and the quality and efficiency in industrial processing will be improved.

2 THEORETICAL ANALYSIS AND CALCULATION

When the femtosecond laser heat the metal films, the electron temperature rises sharply and transfer through thermal diffusion. The nonequilibrium state of the electron temperature and lattice temperature in thermal transfer process is simulated by the double temperature equation [10, 11]:

$$C_e \frac{\partial T_e}{\partial t} - \frac{\partial}{\partial x}(k_e \frac{\partial T_e}{\partial x}) = S(x,t) - G(T_e - T_l) \tag{1}$$

$$C_l \frac{\partial T_l}{\partial t} = G(T_e - T_l) \tag{2}$$

$$T_e(x,0) = T_l(x,0) = 300K \ . \tag{3}$$

$$\frac{\partial T_e}{\partial t} = \frac{\partial T_l}{\partial t} = 0 \ , \tag{4}$$

where C_e is the electron heat capacity, C_l is the lattice heat capacity, T_e is the electron temperature, T_l is the lattice temperature, k_e is the electron thermal conductivity and G is the electron lattice coupling coefficient. Where C_e and k_e in Equation (1) are functions of electron temperature and lattice temperature; the specific expression is

$$C_e = \gamma T_e \ . \tag{5}$$

$$k_e = k_0 \frac{T_e}{T_l} \ . \tag{6}$$

S(x,t) is the heat source under the irradiation of a Gauss laser pulse:

$$S(x,t) = \frac{(1-R)J}{t_p \alpha} \mathrm{e}^{-\beta(\frac{t-t_p}{t_p})^2} \mathrm{e}^{-\frac{x}{\alpha}} \tag{7}$$

where R is the reflectance of the metal surface, J is the laser energy *per* unit area, t_p is the duration of the laser pulse, α is the absorption depth of the metal to the laser energy, β is the coefficient and the value is *4ln2*.

Under femtosecond laser heating, the electron temperature and lattice temperature distribution in 200 nm Cu film are simulated by finite element method. The physical properties of Cu during the simulation are listed in Table 1.

TABLE 1
Physical properties of Cu [12].

γ	k_0	R	α	C_1	G
96.6 J/ m^3K^2	401 W/mK	0.6	14.2 nm	3.5×10^6 J/m^3K	1.02×10^6 W/m^3K

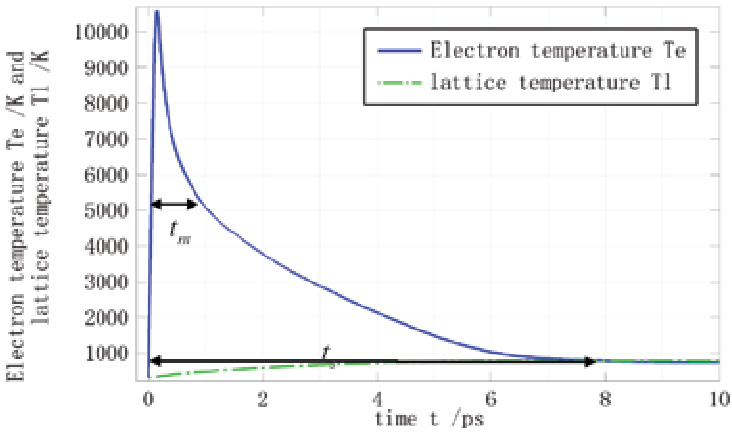

FIGURE 1
Graph of the electron and lattice temperature distribution of the Cu film under single femtosecond laser pulse heating.

3 INTERPRETATION OF RESULTS

As shown in Figure 1, the thickness of the Cu film is 200 nm, the femtosecond laser pulse width is 100 fs and its energy density is 500 J/m^2. The variation of electron temperature and the lattice temperature in the Cu film surface is detected during the laser pulse heating. It can be seen from the Figure 1 that the electron temperature increased fast after the laser beam interaction and reached at the peak of 11000 K. Thereafter it decreased rapidly, while the lattice temperature increased slightly and remained below 1000 K. The electron nonequilibrium relaxation time (t_s) in the Cu film is about 8 ps. In addition, we define the total time interval of the electron temperature from the peak to the half of the peak is full width at half maximum (FWHM) time (t_m). When the femtosecond laser beam can cause the Cu film to produce plasma expansion and effectively remove the metal materials, we find that t_m is very short, about 1 ps, so the processing efficiency of femtosecond laser using single pulse will be not high.

Figure 2 presents the increasing of t_s and t_m by changing the laser pulse width. We simulated the distributions of the electron temperature and lattice temperature with the pulse widths of 50, 100, 200, 350 and 500 fs. Under the condition of pulse width of 50 fs, t_s is 8 ps, t_m is 1 ps, the peak of electron temperature is 11900 K; and under the condition of pulse width is 500 fs, t_s is 8 ps and t_m is 1.5 ps, the peak of electron temperature is 7600 K. It can be clearly seen that: as the pulse width increases, t_s

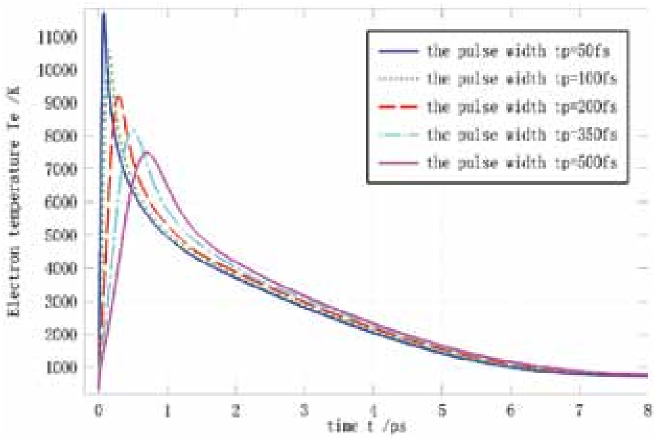

FIGURE 2
Graph of the electron temperature curves under different femtosecond laser pulse widths.

remains unchanged at 8 ps and t_m increases from 1 ps to 1.5 ps. Otherwise, in the condition of the power density of the femtosecond laser remain the same, the electron peak temperature has decreased, inverse to the laser pulse width.

But, t_s and t_m cannot be increased continuously by changing the pulse width, because with the pulse width increases, the laser pulse is no longer a femtosecond pulse, and when the pulse width is greater than the electron relaxation time, there will be significant thermal effect, so as follow we will discuss the increasing of the electron nonequilibrium time by applying a plurality of femtosecond pulses.

Figure 3(a) shows the 200 nm Cu film heating by the two pulses with the single femtosecond laser pulse width is 100 fs. The two laser pulses interval time is very short, only 120 fs, so the electron temperature curve appears as a single peak and its shape similar to the Figure 1. The peak electron temperature is 13500 K, t_s is 10.1 ps and t_m is 1.7 ps. Then, as the pulses interval increases (the pulses interval is 320 fs), two peaks appear in the electron temperature curve and while t_s is substantially unchanged, t_m increases. When the pulses interval is 520 fs, t_s remains unchanged at 10.1 ps, but t_m increases to 2.2 ps. Similarly, from Figure 3(b) and Figure 3(c) it can be seen that when the laser pulse width is 200 and 300 fs, respectively, the two pulses interval increase from 120 to 520 fs, respectively; t_s is basically maintained at 10.1 ps and t_m increases from 1.7 to 2.6 ps. In comparison with Figures 3(a) to (c), it can be seen that the magnitude of the t_s is independent of both the pulses interval and the pulse

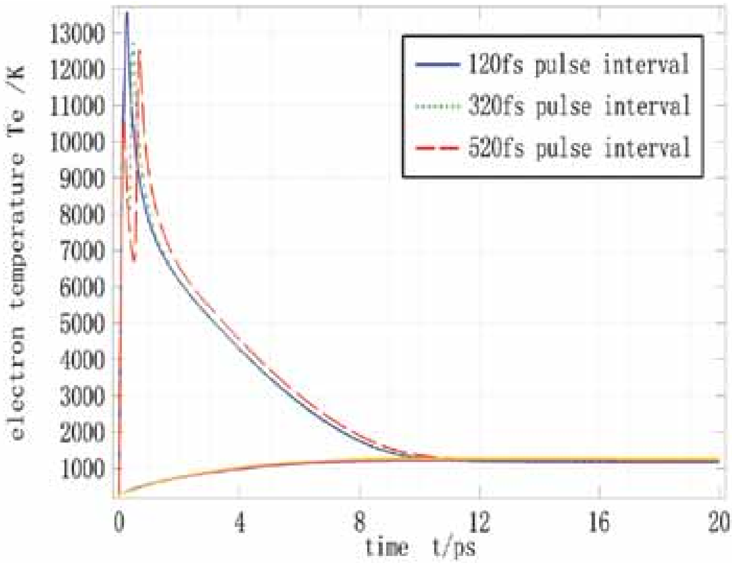
13000
12000
11000
10000
9000
8000
7000
6000
5000
4000
3000
2000
1000
electron temperature Te /K
120fs pulse interval
320fs pulse interval
520fs pulse interval
0
4
8
12
16
20
time t/ps

(a)

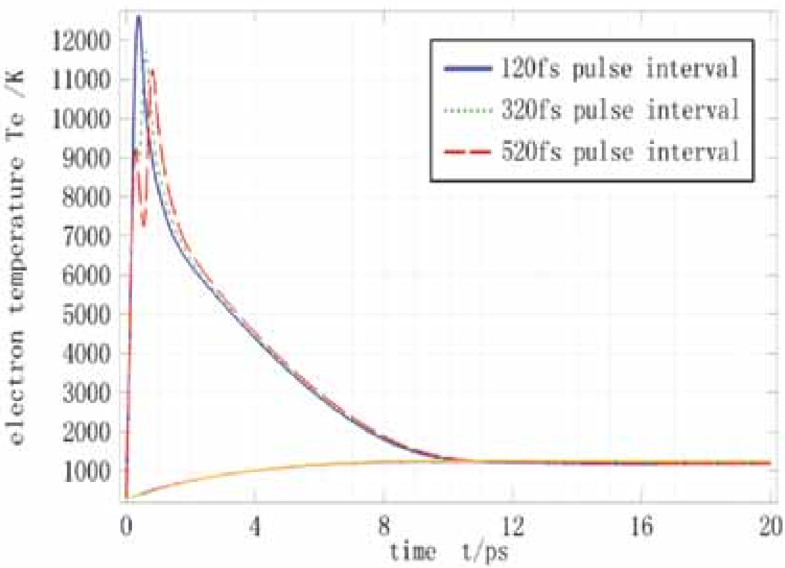
12000
11000
10000
9000
8000
7000
6000
5000
4000
3000
2000
1000
electron temperature Te /K
120fs pulse interval
320fs pulse interval
520fs pulse interval
0
4
8
12
16
20
time t/ps

(b)

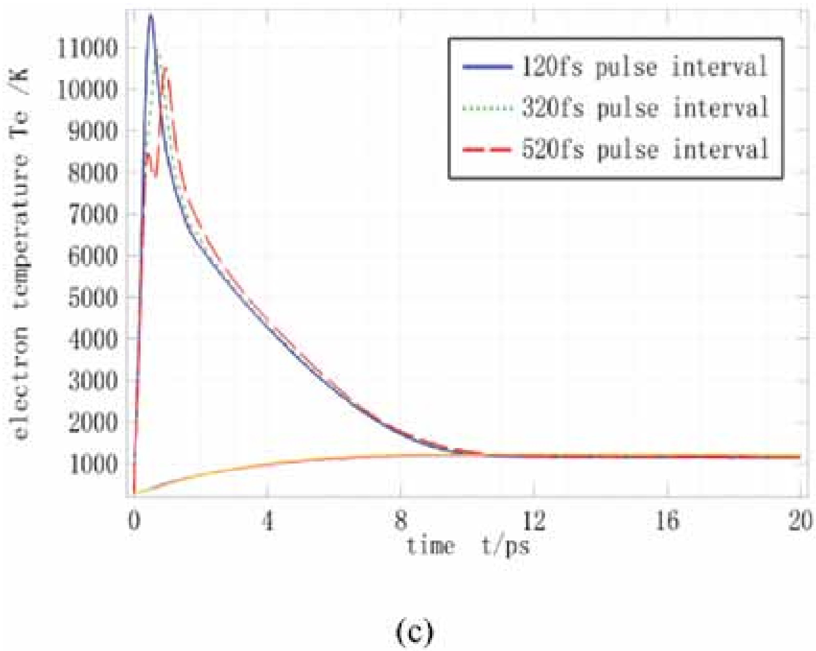

FIGURE 3
Graphs showing the electron and lattice temperature curves irradiated by double femtosecond laser pulses with different width and interval: (a) pulse width is 100 fs; (b) pulse width is 200 fs; and (c) pulse width is 300 fs.

width; however, the t_m value is proportional to the single pulse width and the pulses interval.

In order to prolong t_m, three and four pulses heating the film are simulated, as shown in Figure 4 and Figure 5. In Figure 4 the Cu film is heated by three femtosecond laser pulses and the pulse width is 100, 200 and 300 fs. The value of t_s is unchanged at 12.7 ps, but t_m increased from 2.7 to 4.1 ps. In Figure 5, using four femtosecond laser pulse heating, and the pulse width is 100, 200 and 300 fs, but t_s is 15 ps and t_m increased from 4.3 to 5.2 ps.

Comparing Figures 3 to 5 we find that t_s increases from 10.1 to 15.0 ps with the increase of the number of pulses. The magnitude of t_s is independent of both pulses interval and pulse width, but proportional to the number of pulses. The value of t_m increases from 2.6 (two pulses heating) to 5.2 ps (four pulses heating) and is greatly improved compared to the 1.0 ps (single pulse heating). We can see then that the value of t_m is relative to the number of pulses, the pulse width, as well as the pulses interval.

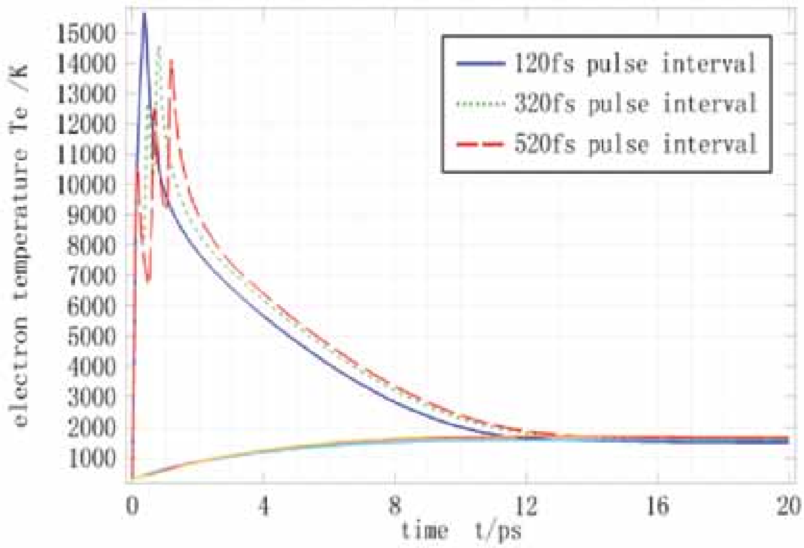
15000
14000
13000
12000
11000
10000
9000
8000
7000
6000
5000
4000
3000
2000
1000
electron temperature Te /K
120fs pulse interval
320fs pulse interval
520fs pulse interval
0
4
8
12
16
20
time t/ps

(a)

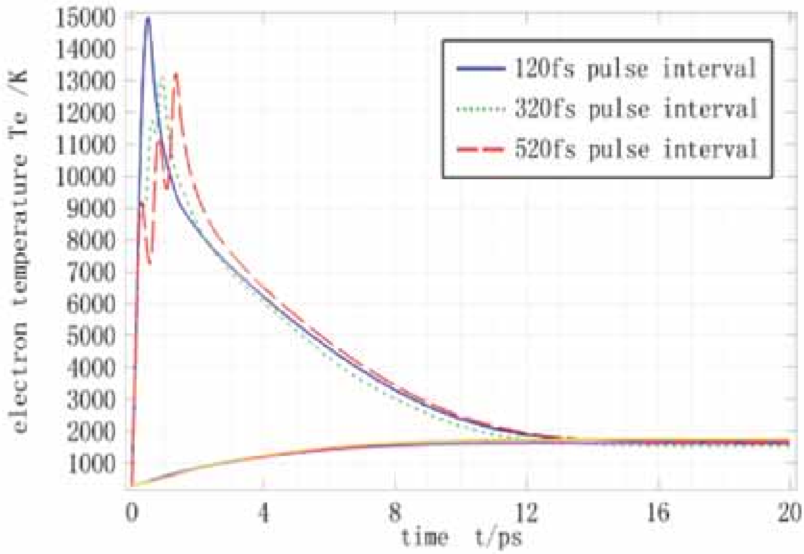
15000
14000
13000
12000
11000
10000
9000
8000
7000
6000
5000
4000
3000
2000
1000
electron temperature Te /K
120fs pulse interval
320fs pulse interval
520fs pulse interval
0
4
8
12
16
20
time t/ps

(b)

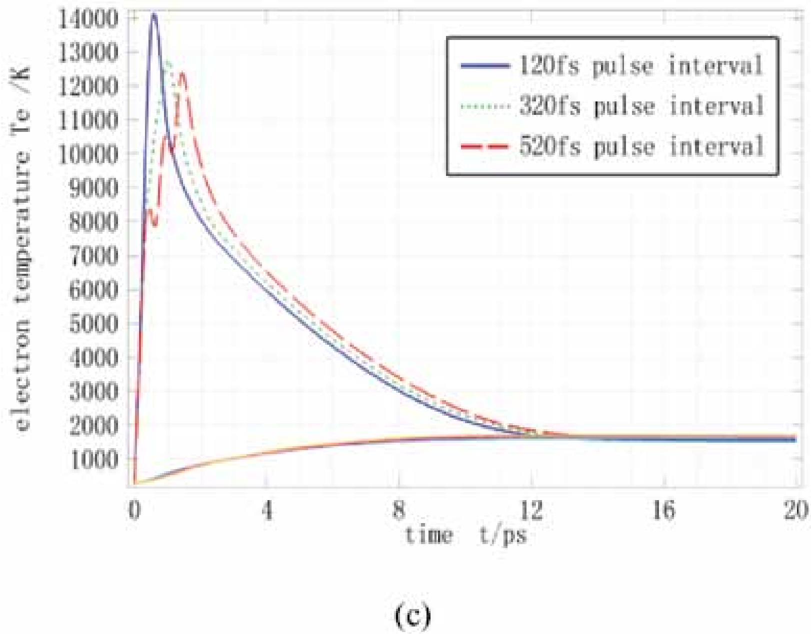

FIGURE 4
Graphs showing the electron and lattice temperature curves irradiated by three femtosecond laser pulses with different width and interval: (a) pulse width is 100 fs; (b) pulse width is 200 fs; and (c) pulse width is 300 fs.

4 CONCLUSIONS

We used a finite element method (FEM) model to simulate electron and lattice temperature, and the nonequilibrium relaxation time changes during the process of femtosecond laser pulses heating of 200 nm Cu metal film. We can find that when the pulse width is 100 fs and the single pulse energy density is 500 J/m^2, the full width at half maximum (FWHM) time of the electron temperature is only about 1.0 ps and the electron nonequilibrium relaxation time is about 8.0 ps. In order to increase the FWHM time and electron nonequilibrium relaxation time we use multiple pulses to excite. The results showed that the FWHM time is proportional to the pulse number, single pulse width and the pulses interval; the electron temperature is independent of the pulses interval and pulse width, but proportional to the number of excitation pulses. Finally, when we use the four femtosecond laser pulses to heat the Cu film with a single pulse width of 300 fs and pulse interval of 520 fs, the FWHM time of electronic temperature is 5.6 ps and the electron nonequilibrium relaxation time is about 15.0 ps. For single pulses the FWHM time of electronic temperature is 1.0 ps and the electron nonequilibrium relaxation time is 8.0 ps. Clearly there has been a significant improvement.

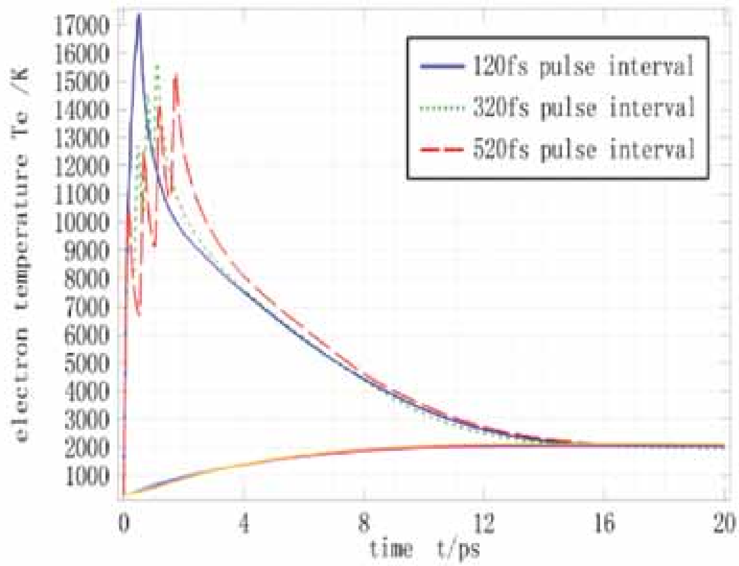
17000
16000
15000
14000
13000
12000
11000
10000
9000
8000
7000
6000
5000
4000
3000
2000
1000
electron temperature Te /K
0
4
8
12
16
20
time t/ps
120fs pulse interval
320fs pulse interval
520fs pulse interval

(a)

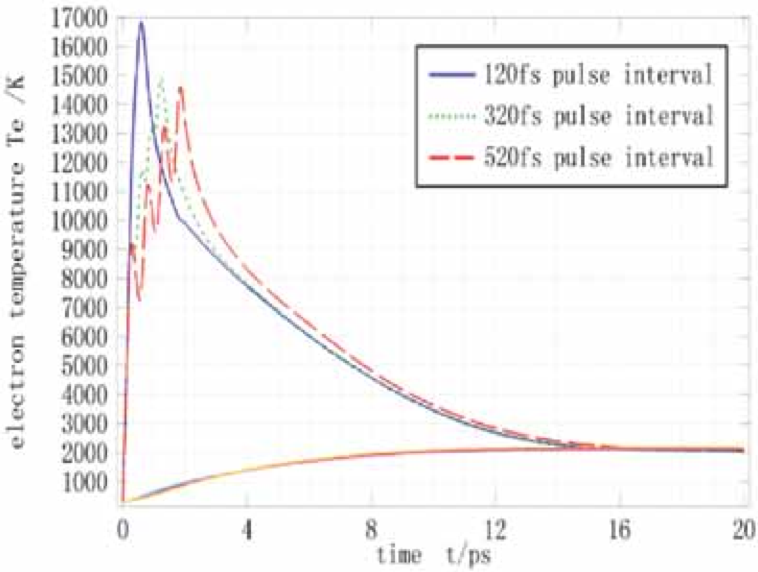
17000
16000
15000
14000
13000
12000
11000
10000
9000
8000
7000
6000
5000
4000
3000
2000
1000
electron temperature Te /K
0
4
8
12
16
20
time t/ps
120fs pulse interval
320fs pulse interval
520fs pulse interval

(b)

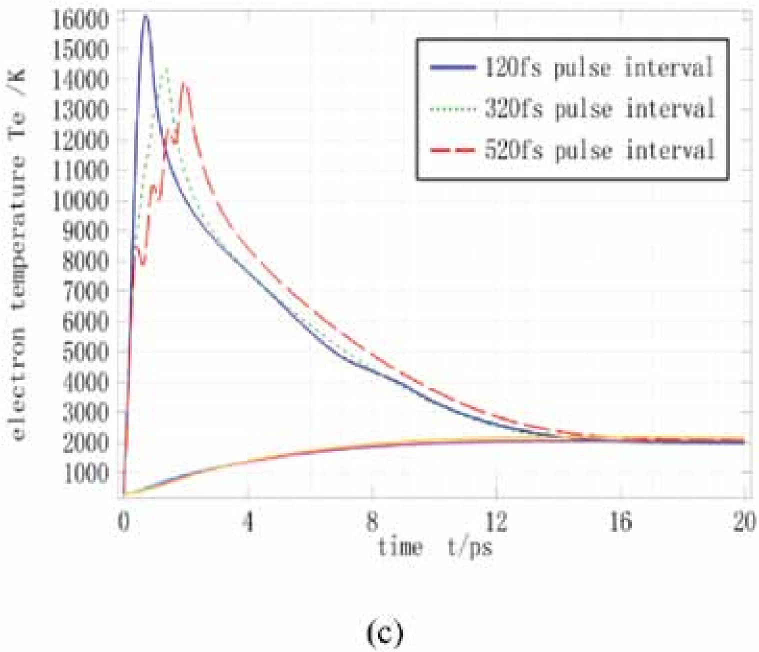

FIGURE 5
Graphs showing the electron and lattice temperature curves irradiated by four femtosecond laser pulses with different width and interval: (a) pulse width is 100 fs; (b) pulse width is 200 fs; and (c) pulse width is 300 fs.

ACKNOWLEDGEMENTS

This work was supported by the National Basic Research Program of China (973 Program) (No. 2011CB013004), The Natural Science Foundation of Jiangsu Province (Youth Fund) (No. BK20150529), the Postdoctoral Science Foundation of China and Jiangsu Province (No. 2015M571678 and No. 1401006B) and the Scientific Research Fund of Senior Professional Talents of Jiangsu University (No. 14JDG072), The National Natural Science Foundation: Research on the electron nonequilibrium heat transfer by mutibeam femtosecond laser controllable excitation and barrier elimination mechanism in metal films.

NOMENCLATURE

C_e	Electron heat capacity (mJ/molK^2)
C_l	Lattice heat capacity (mJ/molK^2)
G	Electron lattice coupling coefficient

J	Laser energy *per* unit area (J/m^2)
k_e	Electron thermal conductivity (W/mK)
R	Reflectance of the Cu surface
t_p	Duration of the laser pulse (seconds)
T_e	Electron temperature (K)
T_l	Lattice temperature (K)

Greek symbols

α	Absorption depth of the laser beam in the Cu (m)
β	Coefficient

REFERENCES

[1] Petkovic D. Prediction of laser welding quality by computational intelligence approaches. *Optik* **140** (2017), 597-600.

[2] Oosterbeek R.N., Ward T., Ashforth S., Bodley O., Rodda A.E. and Simpson M.C. Fast femtosecond laser ablation for efficient cutting of sintered alumina substrates. *Optics & Lasers in Engineering* **84** (2016), 105-110.

[3] Wei J., Ye Y., Sun Z., Liu L. and Zou G. Control of the kerf size and microstructure in Inconel 738 superalloy by femtosecond laser beam cutting. *Applied Surface Science* **370** (2016), 364-372.

[4] Xia B., Jiang L., Li X.W., Yan X.L. and Lu Y.F. Mechanism and elimination of bending effect in femtosecond laser deep-hole drilling. *Optics Express* **23**(21) (2015), 27853-27864.

[5] Straub M., Ventura M. and Gu M. Microvoid channel polymer photonic crystals with large infrared stop gaps and a multitude of higher-order bandgaps fabricated by femtosecond laser drilling in solid resin. *Thin Solid Films* **453-454** (2004), 506-512.

[6] Yavtushenko I.O., Yavtushenko M.S., Zolotovskii I.O., Novikov S.G. , Berintsev A.V., Kadochkin A.S., Stoliarov D.A., Kostishko B.B. and Bunakov N.A. Features of metal surface structuring by high-power femtosecond laser pulses. *Technical Physics Letters* **41**(8) (2015), 743-746.

[7] Ionin A.A., Kudryashov S.I., Makarov S.V., Rudenko A.A., Seleznev L.V., Sinitsyn D.V and Emel'yanov V.I. Nonlinear optical dynamics during femtosecond laser nanostructuring of a silicon surface. *Laser Physics Letters* **12**(12) (2015), 025902.

[8] Tan C., Sun X.Y., Yin K., Luo Z, Xia G.C., Deng W., Zhou J.X. and Duan J. A Surface roughness of cutting metal by femtosecond laser. *Journal of Central South University (Science and Technology)* **42**(12) (2015), 4481-4487.

[9] Li R., Yang X.J., Zhao W., He B, Li M., Zhao H.L. Zhu W.Y. and Wang N. Effect of femtosecond laser micromachining on the roughness of cladding sidewalls. *Infrared and Laser Engineering* **44**(11) (2015), 3244-3249.

[10] Chen A.M., Gao X., Jian Y.F. Ding D.J. and Jin M.X. Numerical solutions and analytical solutions of thermal distribution of ultrashort-pulse laser ablation metal target. *Journal of Atomic and Molecular Physics* **26**(4) (2009), 683-687.

[11] Chen A.M., Jian Y.F., Liu H., Jin M.X. and Ding D.J. Numerical simulation of femtosecond laser ablation by two-temperature model. *Laser & Infrared* **42**(8) (2012), 847-851. (in Chinese)

[12] Christensen B.H., Vestentoft K. and Balling P. Short pulse ablation rates and the two-temperature model. *Applied Surface Science* **253**(15) (2007), 6347-6352.